Asymmetric resonant light absorption in a chloroplast microstructure

Pavel S. Pankin,[1,2,*] **Alexandr V. Shabanov,**[1] **Dmitrii N. Maksimov,**[1,2]
Stepan V. Nabol,[1,2] **Daniil S. Buzin,**[1,2] **Aleksey I. Krasnov,**[1,2] **Gavriil A. Romanenko,**[1,3]
Vitaly S. Sutormin,[1,2] **Vladimir A. Gunyakov,**[1] **Fyodor V. Zelenov,**[3,4]
Albert N. Masyugin,[3,4] **Vladimir P. Vyatkin,**[5] **Ivan V. Nemtsev,**[1,2,5]
Mikhail N. Volochaev,[1,3] **Stepan Ya. Vetrov,**[1,2] **and Ivan V. Timofeev**[1,2]

[1]*Kirensky Institute of Physics, Krasnoyarsk Scientific Center, Siberian Branch, Russian Academy of Sciences, Krasnoyarsk, 660036, Russia*
[2]*Siberian Federal University, Krasnoyarsk, 660041, Russia*
[3]*Siberian State University of Science and Technology, Krasnoyarsk, 660037, Russia*
[4]*AO NPP Radiosvyaz, Krasnoyarsk, 660021, Russia*
[5]*Krasnoyarsk Scientific Center, Siberian Branch, Russian Academy of Sciences, Krasnoyarsk, 660036, Russia*
*Corresponding author: pavel-s-pankin@iph.krasn.ru

It is shown that in the chloroplast periodic structure with a defect, the resonant absorption of light can be implemented. It is found that the resonant light absorption depends significantly on the position of a defect. In terms of the absorption of light energy, an asymmetric resonator is more efficient than a symmetric one. © 2022 Optica
Publishing Group

1. INTRODUCTION

Photosynthesis is the most important global biological process that converts solar energy into chemical energy of organic compounds feeding most living organisms [1]. It replenishes the atmosphere with oxygen [2] and paves a way to creation of alternative energy sources based on the photosynthetic apparatus of plants and bacteria [3,4].

The first phase of photosynthesis is the absorption of light by a chloroplast. It was found by electron microscopy [5] that chloroplasts and related plastids (iridoplasts, bisonoplasts, lamelloplasts, and others) have a periodic microstructure formed by alternating grana separated by stromal partition gaps. In some species of plants and green algae, the optical length of the microstructure period is of the same order of magnitude as the wavelength of visible light; therefore, such microstructures can be called photonic crystals (PhCs) [6,7]. Bragg diffraction of light on PhCs in plant and green algae cells causes the occurrence of photonic bandgaps, which manifest themselves in the spectra as reflection bands determining the structural color and iridescence of cells [8]. In [9–14], the spectral features of chloroplasts and related plastids were interpreted from the viewpoint of PhC optics.

Finite sizes of the plant cell PhCs and their inhomogeneity allow the existence of localized modes, which can be observed in the spectra as resonances in the photonic bandgap. Jacobs *et al.* [9] demonstrated the enhancement of light absorption in the begonia iridoplast structure by means of the PhC edge mode. Geometric parameters of PhCs in plant cells can change dynamically depending on growth [15–22] and illumination conditions [23–28]; these changes are reflected in the transformation of the spectral properties of PhCs [12,13,29]. A change in the optical properties of PhC materials in plant cells causes a change in their spectral properties. For example, Capretti *et al.* [12] demonstrated the effect of the chlorophyll concentration in the thylakoid membrane on the spectral properties of a 2D PhC in higher-plant chloroplasts. The microphotographs reported in [30,31] indicate the presence of starch granules embedded in the PhC of chloroplasts. The starch granules, thus, can be viewed as defects in the crystalline structure. In [29,32], an increase in the density of photonic states at PhC defect mode wavelengths was discussed.

In this paper, we discuss the resonant absorption of light in a periodic PhC structure of a chloroplast with a defect. The key question to be addressed in this paper is whether the stromal gap in chloroplast grana can affect the optical properties and, consequently, have an impact on the absorption of light. The dependence of the resonance absorption coefficient on the position of a defect in the chloroplast PhC is investigated. The results of the numerical simulation are confirmed by theoretical analysis and experimental spectra of an asymmetric microcavity simulating a real biological PhC structure.
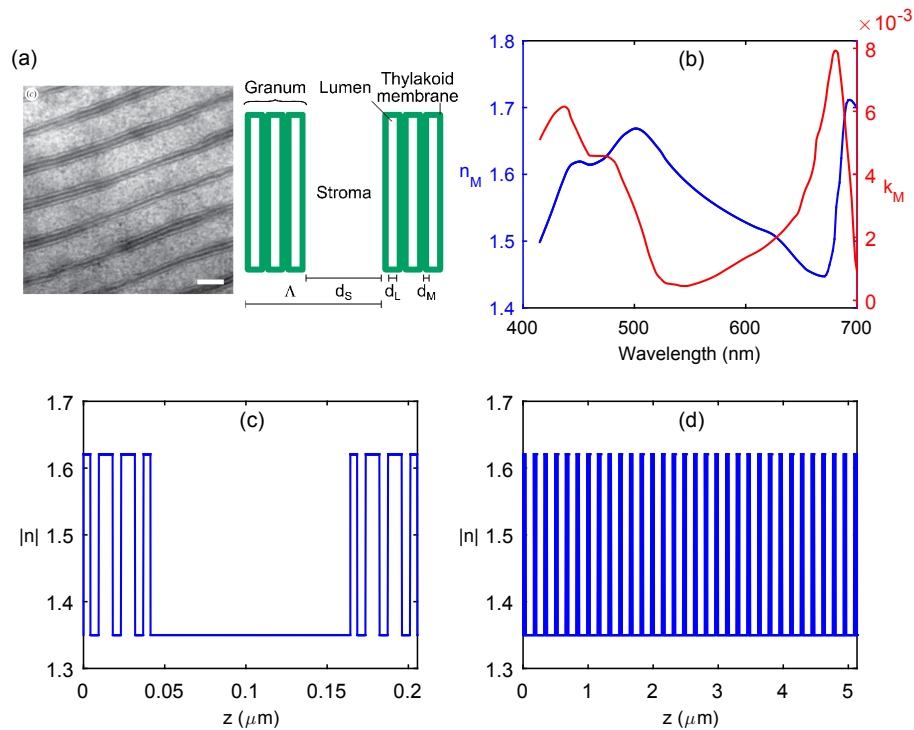
Fig. 1. (a) (left) Electron microscopy image of the bizonoplast *Selaginella erythropus* microstructure (scale bar is 100 nm) [Fig. 2(c) in [11]] and (right) model of the bizonoplast *Selaginella erythropus* layered structure [11]. (b) Complex refractive index $\tilde{n}_M(\lambda) = n_M + i k_M$ of the thylakoid membrane. (c) Refractive index distribution within two neighboring grana ($\lambda = 470$ nm). (d) Refractive index distribution over the whole photonic crystal structure.

2. MODEL

Figure 1(a) shows a model of a 1D PhC representing the chloroplast microstructure. The PhC unit cell is formed by a granum and a stromal gap between two grana. The geometric parameters of the layers correspond to bizonoplasts of *Selaginella erythropus* [11,13]: $d_M = 4.28$ nm, $d_L = 5.2$ nm, and $d_S = 123$ nm. Each granum consists of three thylakoids, including a luminal gap bounded by a membrane on both sides. The refractive index of the luminal n_L and stromal n_S fluid corresponds to an aqueous solution of proteins: $n_L = n_S = 1.35$ [12]. The complex refractive index $\tilde{n}_M(\lambda) = n_M + i k_M$ of the membrane [33], which depends strongly on light wavelength λ, was taken assuming the low concentration of chlorophyll molecules [12], i.e., with the reduced imaginary part k_M [Fig. 1(b)]. The distribution of the refractive index within two neighboring grana is presented in Fig. 1(c); it can be seen that the structure period $\Lambda = 6 d_M + 3 d_L + d_S = 164.3$ nm is comparable to the visible light wavelength. The total number $N = 31$ of structure periods plus one unpaired granum forms a 1D PhC with the refractive index distribution over the structure shown in Fig. 1(d).

3. RESONANCE LIGHT ABSORPTION IN A CHLOROPLAST WITH A DEFECT

Figure 2(a) shows a chloroplast periodic structure. The transmittance, reflectance, and absorptance spectra presented in Figs. 2(b) and 2(d) were calculated by the transfer matrix method [34,35]. It can be seen in Fig. 2(b) that at the low absorptance of the thylakoid membrane, the spectra contain a distinct reflection band corresponding to the photonic bandgap [7]. The center of this band is located at a wavelength of about 450 nm and its width is about 40 nm. In this case, the absorptance increases at resonant wavelengths corresponding to the peaks in the transmittance spectrum. The 1D resonances allow one to increase the light energy density. As an example, Fig. 2(c) shows the electric field intensity distribution normalized to the incident wave energy density at the PhC edge mode wavelength.

The existence of a defect layer corresponding to the decreased stromal gap in one of the unit cells leads to a significant change in the spectra of the structure [Fig. 2(d)]. A resonant dip corresponding to the PhC defect mode emerges in the reflection band. The edge mode shifts to the red end of the spectrum. As can be seen from the absorptance spectrum, the existence of a defect mode leads also to the resonant absorption of light. The resonance line of the defect mode is narrower [Fig. 2(d)] than the line of the edge mode [Fig. 2(b)]. This increases the energy density at the defect mode wavelength [Fig. 2(e)].

Let us now consider the transformation of the spectra of the structure [Figs. 3(a)–3(c)] with a change in the position N_D [Fig. 2(a)] of the defect layer in the PhC. The transmittance spectrum [Fig. 3(a)] is symmetric with respect to the position $N_D = 16$ corresponding to a defect located exactly in the middle of the structure. Since we investigate nonmagnetic substances with a linear optical response, the transmittance spectrum remains unchanged in this case, due to the Lorentz reciprocity [36]. At the same time, the reflectance spectra [Fig. 3(b)] and absorptance spectra [Fig. 3(c)] do not have this symmetry: at the defect mode resonant wavelength, one can see a pronounced
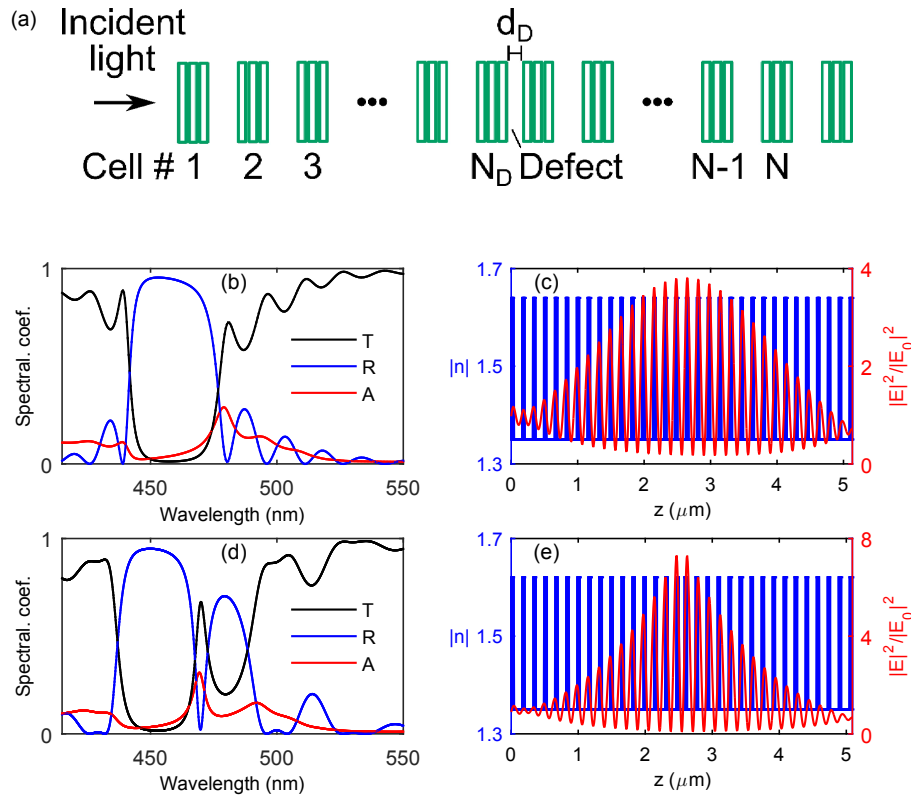
Fig. 2. (a) Model of the chloroplast periodic structure with a defect. Transmittance (black), reflectance (blue), and absorptance (red) spectra of the structure (b) without a defect and (d) with a defect in the middle ($N_D = 16$, $d_D = 0.65d_S$). Distributions of the refractive index and light wave electric field energy density (c) at the edge mode wavelength ($\lambda = 481$ nm) for the structure without a defect and (e) at the defect mode wavelength ($\lambda = 470$ nm) for the structure with a defect in the middle ($N_D = 16$, $d_D = 0.65d_S$).

extremum corresponding to the defect position $N_D = 12$. Here, the reflectance is zero and the absorptance is at maximum, i.e., the critical coupling of the incident wave to the resonance mode is achieved [37,38]. Along with the absorptance, the energy density attains its maximum value at $N_D = 12$ [Fig. 3(d)].

The results obtained can be explained within the temporal coupled-mode theory (TCMT) [39–41]. Let us consider the problem of resonance absorption in an asymmetric resonator [Fig. 3(e)]. According to the TCMT, the amplitude a of the resonant mode with eigenfrequency ω_0 satisfies the following equation:

$$\frac{da(t)}{dt} = -(i\omega_0 + \gamma_0 + \gamma_1 + \gamma_2)a(t) + \sqrt{2\gamma_1}s_1^{(+)}(t). \quad \text{(1)}$$

Here, γ_0 is the rate of energy absorption due to the material loss in the thylakoid membrane; $\gamma_{1,2}$ is the radiative loss rate to waveguides, which is controlled by the PhC mirrors located on the sides of the defect layer (PhC1 and PhC2); and $s_1^{(+)}(t)$ is the amplitude of the light wave incident onto PhC1. The squared absolute value of the amplitude $|a|^2$ is proportional to the energy stored in the resonant mode. For the sinusoidal wave $s_1^{(+)} = e^{-i\omega t}$ at the resonant frequency $\omega = \omega_0$, Eq. (1) leads to the following result:

$$|a(\omega_0)|^2 = \frac{2\gamma_1}{(\gamma_0 + \gamma_1 + \gamma_2)^2}. \quad \text{(2)}$$

Then, the absorptance at the resonant frequency can be determined as

$$A = 2\gamma_0|a(\omega_0)|^2. \quad \text{(3)}$$

Equation (3) explains why the light wave energy density [Fig. 3(d)] and the absorptance [Fig. 3(c)] attain the maximum and minimum simultaneously. The rates of radiative loss through PhC1 and PhC2 are determined by the number of their periods $N_1 = N_D - 1$ and $N_2 = N - N_D$ and can be expressed as $\gamma_{1,2} = e^{-\alpha N_{1,2}}$. Two fitting parameters γ_0 and α of the TCMT model can be estimated from the width of the resonance lines calculated with and without the imaginary part of the refractive index [37].

Equation (2) yields qualitative agreement with the calculated energy density values [Fig. 3(d)]. At $N_D \ll N/2$ ($N_D \gg N/2$), we obtain large γ_1 (γ_2) values. In this case, the resonant quality factor $Q = \omega_0/2(\gamma_0 + \gamma_1 + \gamma_2)$ becomes small, which leads to an increase in the error in the TCMT data [7]. In addition, the differences are caused by the fact that the TCMT equation in the form of Eq. (1) is strictly valid only under the condition of purely resonant absorption, when the absorption off-resonance is zero. Equation (2) contains the radiative loss rate γ_1 in both the numerator and denominator, which explains the extremum in Fig. 3(d) at $N_D = 12$. This suggests that, for the maximum defect mode amplitude, the defect should be, on one hand, close enough to the source to enhance the coupling of incident
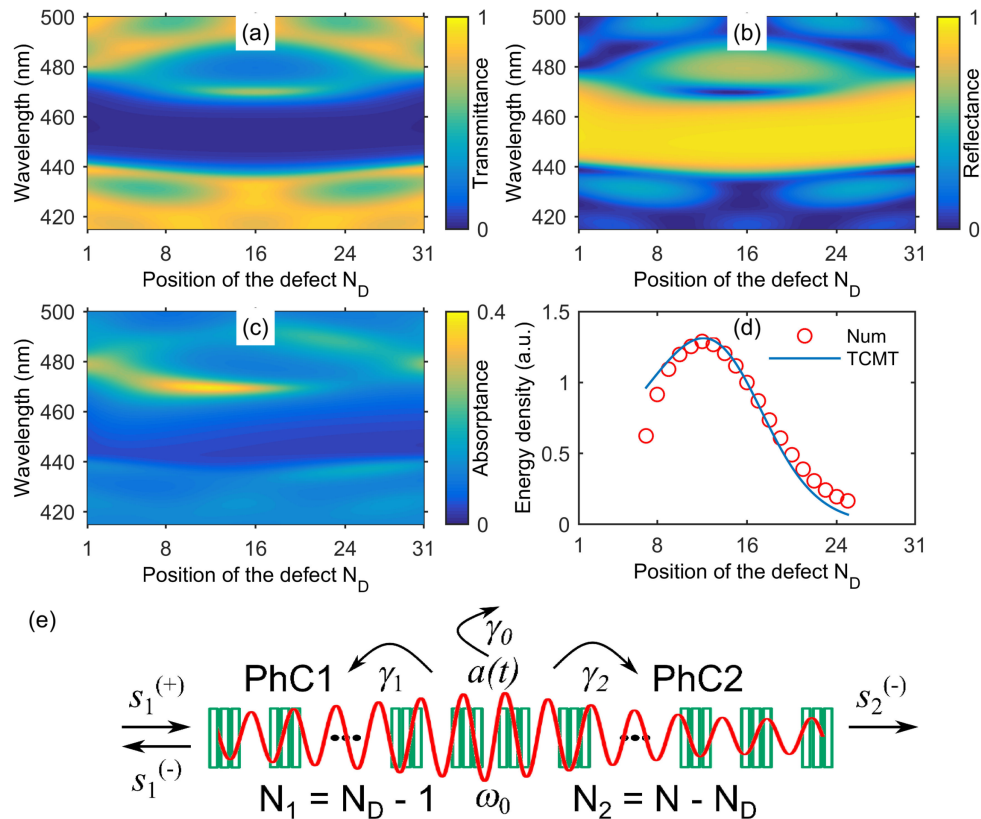
Fig. 3. Spatial symmetry breaking in the chloroplast structure increases the absorption. (a) Transmittance, (b) reflectance, and (c) absorptance spectra. (d) Light wave energy density $w = (\varepsilon|\boldsymbol{E}|^2 + |\boldsymbol{H}|^2)/2$ at the defect mode wavelength calculated by the transfer matrix method at the center of the defect layer (circles) and using Eq. (2) (solid line) ($\gamma_0 = 0.0089, \alpha = 0.1476$). (e) TCMT model.

light and, on the other hand, far enough in the PhC depth to minimize the radiative energy loss rate.

4. EXPERIMENTAL EVIDENCE FOR ASYMMETRIC ABSORPTION AND REFLECTION

The dependence of resonance absorption on the position of a defect in a PhC was demonstrated experimentally in an asymmetric optical microcavity. The microcavity was fabricated in the following stages. First, the PhC mirrors are grown by depositing alternating layers of silicon nitride (Si_3N_4) and silicon oxide (SiO_2) with respective thicknesses of $d_1 = 60$ nm and $d_2 = 86$ nm onto a glass substrate. The alternating layers were formed by plasma-enhanced chemical vapor deposition. One PhC mirror contains three alternating layers and the other, seven layers [Fig. 4(a)]. Second, the PhC mirrors are glued together with a UV glue mixed with spherical spacers to maintain resonator layer thickness of about $d_3 \approx 370$ nm [Fig. 4(b)]. Third, the resonator layer is filled with a solution of a rhodamine 6G dye in dimethyl sulfoxide (DMSO) in concentration 0.0005 M/l by the capillary method [Fig. 4(b)].

The scheme for measuring the spectrum is shown in Fig. 4(c). The spectra of the PhC mirrors and the microcavity were measured under illumination of the samples with a white light source with a Thorlabs OSL2 halogen lamp through an optical fiber (1) attached to the source with a collimator (2) focusing the light on the sample (3) into a beam 3 mm in diameter. The

transmitted or reflected beams were collected by a lens (4) into an optical fiber collimator (5) connected to an Ocean FX-UV-VIS spectrometer. The reflectance spectra were measured using a beam splitter (6) and a silver mirror (7) as a reference. The asymmetric microcavity under study is a PhC with a defect; the defect position changes from $N_D = 2$ to $N_D = 4$, depending on the side from which the microcavity is illuminated [Fig. 4(d)]. Thus, the fabricated microcavity simulates the real biological PhC structure of the chloroplast [Fig. 2(a)].

The spectrum of the PhC mirror with seven layers [Fig. 5(a)] contains a reflection band in the wavelength range of 450–650 nm, which corresponds to the PhC bandgap. The transmittance spectra of the microcavity [Fig. 5(b)] do not depend on the side of light incidence. In the spectral region of the photonic bandgap, there is a resonant peak of the PhC defect mode. The reflectance spectra [Fig. 5(c)] contain a resonant dip at the same wavelength. The depth of the dip depends on the side from which the microcavity is illuminated. The spectra of the PhC mirrors [Fig. 5(d)] and microcavity [Figs. 5(e) and 5(f)] calculated by the transfer matrix method are consistent with the measured spectra. In the numerical calculation, we used the experimental dispersion curves of the complex refractive indices of SiO_2 [42], Si_3N_4 [43], DMSO [44], and rhodamine 6G [45]. The numerical spectra were averaged over the inhomogeneous defect layer thickness $d_3 = 370 \pm 20$ nm, since the precise plane–parallel adjustment was impossible and the
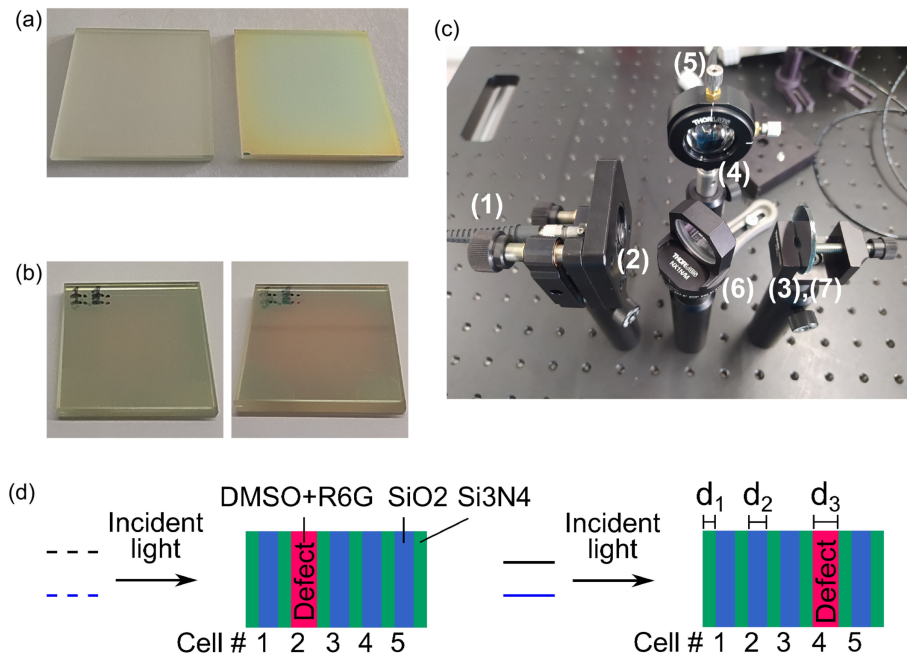
Fig. 4. (a) Photograph of a PhC mirror with three (left) and seven (right) layers. (b) Photograph of the microcavity before (left) and after (right) the filling. (c) Scheme for measuring the microcavity spectra. (d) Microcavity model.
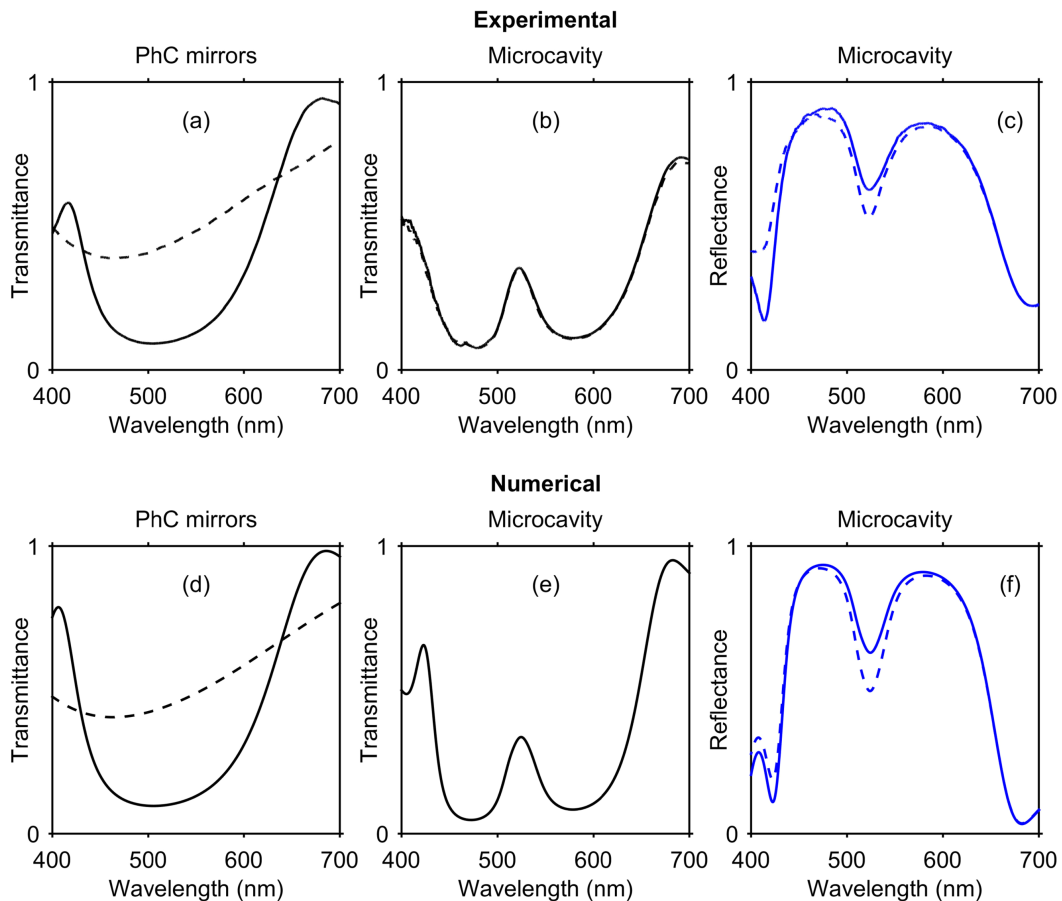
Fig. 5. Experimental and numerical results. (a) Measured and (d) calculated transmittance spectra of the PhC mirrors. (b) Measured and (e) calculated transmittance spectra of the microcavity illuminated from different sides. (c) Measured and (f) calculated reflectance spectra of the microcavity illuminated from different sides. Dotted lines correspond to the incidence of light onto the PhC with three layers and solid lines with seven layers [Fig. 4(d)].

light beam had a finite radius. According to the energy conservation law, the reduced resonant reflection corresponds to the enhanced resonant absorption, which demonstrates the significant dependence of the latter on the position of a defect in the PhC.

5. CONCLUSION

We calculated the scattering and absorbtion spectra as well as the light field distribution for the periodic PhC structure mimicking that of a chloroplast with a stroma defect using the transfer matrix method. The effect of the resonant absorption of light at a wavelength corresponding to the PhC defect mode was demonstrated. A significant dependence of the resonant absorptance on the position of a defect in the chloroplast was demonstrated. The presence of an extremum in the absorptance spectra was explained theoretically within the model based on the TCMT. An asymmetric microcavity simulating the real biological PhC structure of the chloroplast was fabricated with application of PhC mirrors. The measured reflectance spectra of the asymmetric microcavity confirmed the significant dependence of the resonant reflection, as well as the absorption, on the position of the defect layer in the PhC. It is found that in terms of the absorption of light energy, an asymmetric resonator is more efficient than a symmetric one. Taking into account the possibility of dynamic changes in the optical and geometric parameters of the PhC in chloroplasts, including the defect position, we can assume a dynamic change in the spectral position and value of the resonant peak of light absorption in the chloroplast. In summary, we hypothesize that the positions of stroma defects in chloroplasts may drastically affect the absorption of light in living plants. We believe that the results presented could serve as a useseful proof-of-principle model that paves a way to better understanding of light absorption mechanisms in chloroplasts.

REFERENCES

1. D. Shevela, L. O. Bjorn, and G. Govindjee, *Photosynthesis: Solar Energy For Life* (World Scientific, 2018).
2. B. Ivanov, M. Kozuleva, and M. Mubarakshina, "Oxygen metabolism in chloroplast," in *Cell Metabolism-Cell Homeostasis and Stress Response* (InTech, 2012), pp. 39–72.
3. E. Musazade, R. Voloshin, N. Brady, J. Mondal, S. Atashova, S. K. Zharmukhamedov, I. Huseynova, S. Ramakrishna, M. M. Najafpour, J.-R. Shen, B. D. Bruce, S. I. Allakhverdiev, B. D. Bruce, and S. I. Allakhverdiev, "Biohybrid solar cells: fundamentals, progress, and challenges," J. Photochem. Photobiol. C **35**, 134–156 (2018).
4. M. D. Mamedov, G. E. Milanovsky, L. Vitukhnovskaya, and A. Y. Semenov, "Measurements of the light-induced steady state electric potential generation by photosynthetic pigment-protein complexes," Biophys. Rev. **14**, 933–939 (2022).
5. H. Kirchhoff, "Chloroplast ultrastructure in plants," New Phytol. **223**, 565–574 (2019).
6. V. F. Shabanov, S. Y. Vetrov, and A. V. Shabanov, *Optics of Real Photonic Crystals: Liquid Crystal Defects* (Irregularities (SB RAS), 2005) [in Russian].
7. J. D. Joannopoulos, S. G. Johnson, J. N. Winn, and R. D. Meade, *Photonic Crystals: Molding the Flow of Light*, 2nd ed. (Princeton University, 2008).
8. S.-H. Pao, P.-Y. Tsai, C.-I. Peng, P.-J. Chen, C.-C. Tsai, E.-C. Yang, M.-C. Shih, J. Chen, J.-Y. Yang, P. Chesson, and C.-R. Sheue, "Lamelloplasts and minichloroplasts in Begoniaceae: iridescence and photosynthetic functioning," J. Plant Res. **131**, 655–670 (2018).
9. M. Jacobs, M. Lopez-Garcia, O.-P. Phrathep, T. Lawson, R. Oulton, and H. M. Whitney, "Photonic multilayer structure of Begonia chloroplasts enhances photosynthetic efficiency," Nat. Plants **2**, 16162 (2016).
10. M. Lopez-Garcia, N. Masters, H. E. O'Brien, J. Lennon, G. Atkinson, M. J. Cryan, R. Oulton, and H. M. Whitney, "Light-induced dynamic structural color by intracellular 3D photonic crystals in brown algae," Sci. Adv. **4**, eaan8917 (2018).
11. N. J. Masters, M. Lopez-Garcia, R. Oulton, and H. M. Whitney, "Characterization of chloroplast iridescence in Selaginella erythropus," J. R. Soc. Interface **15**, 0559 (2018).
12. A. Capretti, A. K. Ringsmuth, J. F. van Velzen, A. Rosnik, R. Croce, and T. Gregorkiewicz, "Nanophotonics of higher-plant photosynthetic membranes," Light Sci. Appl. **8**, 5 (2019).
13. M. A. Castillo, W. P. Wardley, and M. Lopez-Garcia, "Light-dependent morphological changes can tune light absorption in iridescent plant chloroplasts: a numerical study using biologically realistic data," ACS Photon. **8**, 1058–1068 (2021).
14. E. Bukhanov, A. V. Shabanov, M. N. Volochaev, and S. A. Pyatina, "The role of periodic structures in light harvesting," Plants **10**, 1967 (2021).
15. A. O. Taylor and J. Rowley, "Plants under climatic stress: I. Low temperature, high light effects on photosynthesis," Plant Physiol. **47**, 713–718 (1971).
16. H. A. Kratsch and R. R. Wise, "The ultrastructure of chilling stress," Plant Cell Environ. **23**, 337–350 (2000).
17. A. N. Uzunova and L. P. Popova, "Effect of salicylic acid on leaf anatomy and chloroplast ultrastructure of barley plants," Photosynthetica **38**, 243–250 (2000).
18. P. Mäkelä, J. Kärkkäinen, and S. Somersalo, "Effect of glycinebetaine on chloroplast ultrastructure, chlorophyll and protein content, and RuBPCO activities in tomato grown under drought or salinity," Biol. Plant. **43**, 471–475 (2000).
19. D. Zhao, D. M. Oosterhuis, and C. W. Bednarz, "Influence of potassium deficiency on photosynthesis, chlorophyll content, and chloroplast ultrastructure of cotton plants," Photosynthetica **39**, 103–109 (2001).
20. J. Molas, "Changes of chloroplast ultrastructure and total chlorophyll concentration in cabbage leaves caused by excess of organic Ni (II) complexes," Environ. Exp. Bot. **47**, 115–126 (2002).
21. F. Bejaoui, J. J. Salas, I. Nouairi, A. Smaoui, C. Abdelly, E. Martinez-Force, and N. B. Youssef, "Changes in chloroplast lipid contents and chloroplast ultrastructure in Sulla carnosa and Sulla coronaria leaves under salt stress," J. Plant Physiol. **198**, 32–38 (2016).
22. Q. Du, X.-H. Zhao, L. Xia, C.-J. Jiang, X.-G. Wang, Y. Han, J. Wang, and H.-Q. Yu, "Effects of potassium deficiency on photosynthesis, chloroplast ultrastructure, ROS, and antioxidant activities in maize (Zea mays L.)," J. Integr. Agric. **18**, 395–406 (2019).
23. H. Kirchhoff, C. Hall, M. Wood, M. Herbstová, O. Tsabari, R. Nevo, D. Charuvi, E. Shimoni, and Z. Reich, "Dynamic control of protein diffusion within the granal thylakoid lumen," Proc. Natl. Acad. Sci. USA **108**, 20248–20253 (2011).
24. H. Kirchhoff, M. Li, and S. Puthiyaveetil, "Sublocalization of cytochrome b6f complexes in photosynthetic membranes," Trends Plant Sci. **22**, 574–582 (2017).
25. R. Ghaffar, M. Weidinger, B. Mähnert, M. Schagerl, and I. Lichtscheidl, "Adaptive responses of mature giant chloroplasts in the deep-shade lycopod Selaginella erythropus to prolonged light and dark periods," Plant Cell Environ. **41**, 1791–1805 (2018).
26. M. Li, R. Mukhopadhyay, V. Svoboda, H. M. O. Oung, D. L. Mullendore, and H. Kirchhoff, "Measuring the dynamic response

of the thylakoid architecture in plant leaves by electron microscopy," Plant Direct **4**, e00280 (2020).

27. J. Liu, S. Li, C. Wu, I. A. Valdespino, J. Ho, Y. Wu, H. Chang, T. Guu, M. Kao, C. Chesson, S. Das, H. Oppenheimer, A. Bakutis, P. Saenger, N. Salazar Allen, J. W. H. Yong, B. Adjie, R. Kiew, N. Nadkarni, C. Huang, P. Chesson, and C. Sheue, "Gigantic chloroplasts, including bizono-plasts, are common in shade-adapted species of the ancient vascular plant family Selaginellaceae," Am. J. Bot. **107**, 562–576 (2020).

28. H. K. Lichtenthaler, C. Buschmann, M. Döll, H.-J. Fietz, T. Bach, U. Kozel, D. Meier, and U. Rahmsdorf, "Photosynthetic activity, chloroplast ultrastructure, and leaf characteristics of high-light and low-light plants and of sun and shade leaves," Photosynth. Res. **2**, 115–141 (1981).

29. A. Shabanov, M. Korshunov, and E. Bukhanov, "Features of the amplification of the electromagnetic field and the density of states of photonic crystal structures in plants," Comput. Opt. **43**, 231–237 (2019).

30. C.-R. Sheue, V. Sarafis, R. Kiew, H.-Y. Liu, A. Salino, L.-L. Kuo-Huang, Y.-P. Yang, C.-C. Tsai, C.-H. Lin, J. W. H. Yong, and M. S. B. Ku, "Bizonoplast, a unique chloroplast in the epidermal cells of microphylls in the shade plant Selaginella erythropus (Selaginellaceae)," Am. J. Bot. **94**, 1922–1929 (2007).

31. C.-R. Sheue, J.-W. Liu, J.-F. Ho, A.-W. Yao, Y.-H. Wu, S. Das, C.-C. Tsai, H.-A. Chu, M. S. B. Ku, and P. Chesson, "A variation on chloroplast development: the bizonoplast and photosynthetic efficiency in the deep-shade plant Selaginella erythropus," Am. J. Bot. **102**, 500–511 (2015).

32. M. A. Korshunov, A. V. Shabanov, E. R. Bukhanov, and V. F. Shabanov, "Effect of long-period ordering of the structure of a plant on the initial stages of photosynthesis," Dokl. Phys. **63**, 1–4 (2018).

33. G. Paillotin, W. Leibl, J. Gapiński, J. Breton, and A. Dobek, "Light gradients in spherical photosynthetic vesicles," Biophys. J. **75**, 124–133 (1998).

34. P. Yeh, "Electromagnetic propagation in birefringent layered media," J. Opt. Soc. Am. **69**, 742–756 (1979).

35. D. S. Bethune, "Optical harmonic generation and mixing in multilayer media: analysis using optical transfer matrix techniques," J. Opt. Soc. Am. B **6**, 910–916 (1989).

36. L. D. Landau, *Electrodynamics of Continuous Media* (Pergamon, 1984).

37. B. Auguié, A. Bruchhausen, and A. Fainstein, "Critical coupling to Tamm plasmons," J. Opt. **17**, 35003 (2015).

38. Z.-Y. Yang, S. Ishii, T. Yokoyama, T. D. Dao, M.-G. Sun, P. S. Pankin, I. V. Timofeev, T. Nagao, and K.-P. Chen, "Narrowband wavelength selective thermal emitters by confined Tamm plasmon polaritons," ACS Photon. **4**, 2212–2219 (2017).

39. S. Fan, W. Suh, and J. D. Joannopoulos, "Temporal coupled-mode theory for the Fano resonance in optical resonators," J. Opt. Soc. Am. A **20**, 569–572 (2003).

40. Z. Zhao, C. Guo, and S. Fan, "Connection of temporal coupled-mode-theory formalisms for a resonant optical system and its time-reversal conjugate," Phys. Rev. A **99**, 33839 (2019).

41. H. A. Haus, *Waves and Fields in Optoelectronics*, Prentice-Hall Series in Solid State Physical Electronics (Prentice Hall, 1983).

42. L. Gao, F. Lemarchand, and M. Lequime, "Refractive index determination of SiO_2 layer in the UV/Vis/NIR range: spectrophotometric reverse engineering on single and bi-layer designs," J. Eur. Opt. Soc.-Rapid Publ. **8**, 8 (2013).

43. K. Luke, Y. Okawachi, M. R. E. Lamont, A. L. Gaeta, and M. Lipson, "Broadband mid-infrared frequency comb generation in a Si_3N_4 microresonator," Opt. Lett. **40**, 4823–4826 (2015).

44. I. Z. Kozma, P. Krok, and E. Riedle, "Direct measurement of the group-velocity mismatch and derivation of the refractive-index dispersion for a variety of solvents in the ultraviolet," J. Opt. Soc. Am. B **22**, 1479–1485 (2005).

45. W. Leupacher and A. Penzkofer, "Refractive-index measurement of absorbing condensed media," Appl. Opt. **23**, 1554–1558 (1984).